Bioorganic Chemistry 91 (2019) 103145

Contents lists available at ScienceDirect

Bioorganic Chemistry

journal homepage: www.elsevier.com/locate/bioorg

Chemical constituents of the root bark of *Ulmus davidiana* var. *japonica* and their potential biological activities

Hae Min So[a,1], Jae Sik Yu[a,1], Zarha Khan[b], Lalita Subedi[b], Yoon-Joo Ko[c], Il Kyun Lee[d], Woo Sung Park[e], Sang J. Chung[a], Mi-Jeong Ahn[e], Sun Yeou Kim[b], Ki Hyun Kim[a,*]

[a] School of Pharmacy, Sungkyunkwan University, Suwon 16419, Republic of Korea
[b] College of Pharmacy, Gachon Institute of Pharmaceutical Science, Gachon University, 191 Hambakmoero, Yeonsu-gu, Incheon 21936, Republic of Korea
[c] Laboratory of Nuclear Magnetic Resonance, National Center for Inter-University Research Facilities (NCIRF), Seoul National University, Gwanak-gu, Seoul 08826, Republic of Korea
[d] Research Center, Natural Medicine Research Team, Richwood Trading Company, LTD, Seoul 08826, Republic of Korea
[e] College of Pharmacy and Research Institute of Pharmaceutical Sciences, Gyeongsang National University, Jinju 52828, Republic of Korea

ARTICLE INFO

Keywords:
Ulmus davidiana var. *japonica*
Ulmaceae
Nerve growth factor (NGF)
Anti-neuroinflammation
Anti-*Helicobacter pylori* activity

ABSTRACT

The root bark of *Ulmus davidiana* var. *japonica* (Ulmaceae), commonly known as yugeunpi, has been used as a traditional Korean medicine for the treatment of gastroenteric and inflammatory disorders. As part of continuing projects to discover bioactive natural products from traditional medicinal plants with pharmacological potential, phytochemical investigation of the root bark of this plant was carried out. This led to the successful isolation of a new chromane derivative (**1**) and 22 known compounds: catechin derivatives (**2–5**), megastigmane glycoside (**6**), dihydrochalcone glycosides (**7** and **8**), flavanone glycosides (**9** and **10**), coumarins (**11** and **12**), lignan derivatives (**13–17**), and phenolic compounds (**18–23**). The structure of the new compound (**1**) was determined with 1D and 2D NMR spectroscopy and HR-ESIMS, and its absolute configurations were achieved by chemical reactions and the gauge-including atomic orbital (GIAO) NMR chemical shifts calculations. All the isolated compounds were evaluated for their potential biological activities including neuro-protective, anti-neuroinflammatory, and anti-*Helicobacter pylori* activities. Among the isolates, compounds **1**, **8**, and **20** displayed stronger potency by causing a greater increase in the production and the activity of nerve growth factor (NGF) in C6 glioma cells (147.04 ± 4.87, 206.27 ± 6.70, and 143.70 ± 0.88%, respectively), whereas compounds **11**, **14**, and **19** inhibited nitric oxide (NO) production in lipopolysaccharide (LPS)-stimulated murine microglial cells (IC_{50} of 18.72, 12.31, and, 21.40 μM, respectively). In addition, compounds **1**, **11**, **18**, and **20** showed anti-*H. pylori* activity with MIC values of 25 or 50 μM against two strains of *H. pylori* 51 and 43504. These findings provide scientific evidence that supports the traditional usage of *U. davidiana* var. *japonica* root bark in the treatment of gastroenteric and inflammatory disorders.

1. Introduction

Ulmus davidiana var. *japonica* (Ulmaceae) is widely distributed in Asian countries [1], and its root bark, well-known as yugeunpi, has been used in Korean traditional medicine to treat gastroenteric disorders (diarrhea, gastritis, enteritis, and gastric cancer) and inflammatory disorders (rheumatoid arthritis, mastitis, and hepatitis) as well as eruption, edema, hemorrhoids, and jaundice [2–5]. Previous pharmacological studies reported that the extracts from this plant showed suppressive effects on collagen-induced arthritis [6], anti-angiogenic activity [7], and modulating effects on immunocompetence [8]. In addition, the bioactive constituents of the root bark extract of *U. davidiana* var. *japonica* are flavonoids [5,9], triterpene esters [4], sesquiterpene-*O*-naphthaquinones [10], lignan and neolignan glycosides [11], and butenyl cyclohexenone glycosides [12]. Of note, flavan-3-ols from *U. davidiana* var. *japonica* inhibited protein glycation [13], and the sesquiterpene *O*-naphthoquinones exerted anti-oxidative effects in rat liver microsomes [10]. In addition, the sesquiterpenes from this plant inhibited lipopolysaccharide (LPS)-induced nitric oxide (NO) production [14]. Taken together, these previously reported findings strongly suggest the potential application of *U. davidiana* var. *japonica* and its bioactive compounds.

* Corresponding author.
E-mail address: khkim83@skku.edu (K.H. Kim).
[1] These authors contributed equally to this work.

https://doi.org/10.1016/j.bioorg.2019.103145
Received 27 April 2019; Received in revised form 2 July 2019; Accepted 20 July 2019
Available online 25 July 2019
0045-2068/

As a part of continuing projects to discover bioactive natural products from traditional medicinal plants that have pharmacological potential [15–21], phytochemical investigation of the root bark of *U. davidiana* var. *japonica* was carried out, and led to the successful isolation of 23 compounds (**1–23**) including a new chromane derivative (**1**). The structure of the new compound was determined with 1D and 2D NMR spectroscopy and HR-ESIMS as well as with chemical reactions and computational method coupled with a statistical procedure (DP4 +). Here, we report the isolation and the structural elucidation of compounds **1–23** and their potential biological activities including nerve growth factor (NGF) production, anti-neuroinflammatory and anti-*Helicobacter pylori* activities, to support the traditional usage of *U. davidiana* var. *japonica* root bark in the treatment of gastroenteric and inflammatory disorders.

2. Experimental

2.1. General experimental procedures

Optical rotations were measured using a Jasco P-2000 polarimeter (Jasco, Easton, MD, USA). Infrared (IR) spectra were recorded on an IFS-66/s FT-IR spectrometer (Bruker, Karlsruhe, Germany). Electronic circular dichroism (ECD) spectra in MeOH were acquired in a quartz cuvette of 1 mm optical path length on a JASCO J-1500 spectropolarimeter (Tokyo, Japan). Ultraviolet (UV) spectra were acquired on an Agilent 8453 UV–visible spectrophotometer (Agilent Technologies, Santa Clara, CA). High-resolution (HR)-electrospray ionization (ESI) mass spectra were recorded on a Waters Xevo G2 quadrupole time-of-flight (QTOF) mass spectrometer (Waters Co., Milford, MA, USA) and Synapt G2 HDMS QTOF mass spectrometer. NMR spectra were measured using a Bruker AVANCE III 800 NMR spectrometer operating at 800 MHz (^{1}H) and 200 MHz (^{13}C) (Bruker). Preparative high-performance liquid chromatography (HPLC) was conducted using a Waters 1525 binary HPLC pump with a Waters 996 photodiode array detector (Waters Corporation, Milford, CT, USA). Semi-preparative HPLC was conducted with a Shimadzu Prominence HPLC System with SPD-20A/20AV series Prominence HPLC UV–vis detectors (Shimadzu, Tokyo, Japan). LC/MS analysis was performed on an Agilent 1200 series HPLC system with a diode array detector and 6130 Series ESI mass spectrometer using an analytical Kinetex C18 100 Å column (100 mm × 2.1 mm i.d., 5 μm) (Phenomenex, Torrance, CA). Column chromatography was performed with silica gel 60, 230–400 mesh, RP-C18 silica gel, 230–400 mesh (Merck, Darmstadt, Germany) and silica Sep-Pak Vac 6 cc and C_{18} Sep-Pak Vac 6 cc cartridges (Waters). The packing material for molecular sieve column chromatography was Sephadex LH-20 (Pharmacia, Uppsala, Sweden). In addition, Diaion HP-20 (Mitsubishi Chemical, Tokyo, Japan) was used for open-column chromatography. Thin-layer chromatography (TLC) was conducted using precoated silica gel F_{254} plates and reverse-phase (RP)-18 F_{254s} plates (Merck). The spots on TLC were detected using UV light and heat after dipping in anisaldehyde-sulfuric acid.

2.2. Plant material

The root barks of *U. davidiana* var. *japonica* (Rehder) Nakai were collected from Wonhwasan-ro, Jecheon-si, Chungcheongbuk-do, Korea in 2016, and purchased by Donggwang General Corporation. The plant was authenticated by one of the authors (K. H. Kim). A voucher specimen (SKKU-NR 0401) of the plant has been deposited at the herbarium of the School of Pharmacy, Sungkyunkwan University, Suwon, Korea.

2.3. Extraction and isolation

The dried root bark of *U. davidiana* var. *japonica* (10 kg) was extracted in 50% aqueous EtOH (60 L) for 2 days at 70 °C and filtered. The filtrate was concentrated under a reduced pressure using a rotavapor to obtain the EtOH extract (900 g). Half of the EtOH extract (300 g) was suspended in distilled water (800 mL), and was successively solvent-partitioned with hexane, dichloromethane (CH_2Cl_2), ethyl acetate (EtOAc), and *n*-butanol (BuOH). Four fractions with increasing polarity—hexane-soluble (4.0 g), CH_2Cl_2-soluble (39.0 g), EtOAc-soluble (25.0 g) and BuOH-soluble fractions (81.0 g), were obtained. By comparison with our house-built UV library, LC/MS analysis of the four fractions from the solvent partitioning indicated the presence of major compounds in the EtOAc-soluble fraction.

The EtOAc-soluble fraction (25 g) was subjected to a Diaion HP-20 column in a gradient solvent system of MeOH (100% H_2O, 20% MeOH, 40% MeOH, 60% MeOH, 80% MeOH, and 100% MeOH) to yield six fractions (E0, E2, E4, E6, E8, and E10). Fraction E4 (4.5 g) was further subjected to silica gel column chromatography (200 g, eluted with CH_2Cl_2/MeOH (20:1 → 1:1), gradient system) to yield seven fractions (E4A–E4G). Fraction E4B (70.9 mg) was separated by Phenomenex Strata SI-1 Silica (55 μm, 70 Å, 2 g/12 mL) cartridge with CH_2Cl_2/MeOH (40:1 → 1:1, gradient system) to yield six fractions (E4B1–E4B6). Fraction E4B4 (23.8 mg) was purified using semi-preparative HPLC (14% MeOH) to yield compound **18** (t_R 68.4 min, 1.0 mg). Fraction E4C (2238.8 mg) was separated by RP-C18 column chromatography with a gradient solvent system of MeOH-H_2O (10–100% MeOH) to yield seven sub-fractions (E4C1–E4C7). Fraction E4C4 (1668.5 mg) was separated by preparative reversed-phase HPLC with a gradient solvent system of MeOH-H_2O (10–80% MeOH) to give four fractions (E4C41–E4C44). Fraction E4C42 (209.5 mg) was separated by semi-preparative HPLC (18% MeOH) to yield compounds **2** (t_R 46.0 min, 69.6 mg), **3** (t_R 37.5 min, 32.9 mg), and **5** (t_R 29 min, 47.0 mg). Fraction E4C6 (24.2 mg) was purified using semi-preparative HPLC with a gradient solvent system of MeOH-H_2O [formic acid 0.1% (v/v)] (21–24% MeOH) to yield compound **6** (t_R 53.0 min, 2.2 mg). Fraction E4C37 (98.4 mg) was separated on Sephadex LH-20 column using a solvent system of 100% MeOH to yield six sub-fractions (E4C71–E4C76). Fraction E4C73 (6.6 mg) was purified using semi-preparative HPLC (28% MeOH) to yield compound **1** (t_R 32.5 min, 2.0 mg). Fraction E4D (4240.7 g) was separated on Sephadex LH-20 column using a solvent system of MeOH-H_2O (50% MeOH) to yield five sub-fractions (E4D1-E4D5). Fraction E4D2 (430.8 mg) was purified using semi-preparative HPLC (18% MeOH) to yield compound **4** (t_R 42.0 min, 20.5 mg). Fraction E4E (3.5 g) was separated by RP-C18 column chromatography with a gradient solvent system of MeOH-H_2O (0–30% MeOH) to yield eleven sub-fractions (E4E1–E4E11). Fraction E4E1 (32 mg) was purified using semi-preparative HPLC (3% MeCN) to yield compound **19** (t_R 42.0 min, 2.2 mg). Fraction E6 (2.6 g) was subjected to silica gel column chromatography [100 g, eluted with CH_2Cl_2/MeOH (50:1 → 1:1), gradient system] to obtain seven fractions (E6A–E6G). Fraction E6A (23.8 mg) was separated by semi-preparative HPLC with a solvent system of MeOH-H_2O [formic acid 0.1% (v/v)] (25% MeOH) to yield six fractions (E6A1–E6A6). Fraction E6B (55.2 mg) was separated by semi-preparative HPLC with a solvent system of MeOH-H_2O [formic acid 0.1% (v/v)] (25% MeOH) to yield six fractions (E6B1–E6B6). Fraction E6A4 (2.3 mg) and E6B4 (5.7 mg) were combined and purified using semi-preparative HPLC with a solvent system of MeCN-H_2O [formic acid 0.1% (v/v)] (13% MeCN) to yield compound **21** (t_R 29.0 min, 2.1 mg). Fraction E6B6 (26.7 mg) was purified using semi-preparative HPLC with a solvent system of MeCN-H_2O [formic acid 0.1% (v/v)] (12% MeCN) to yield compound **20** (t_R 33.5 min, 1.5 mg). Fraction E8 (1100 mg) was separated by preparative reversed-phase HPLC with a gradient solvent system of MeOH-H_2O (45–100% MeOH) to give six fractions (E8A–E8F). Fraction E8B (192.1 mg) was separated on Sephadex LH-20 column using a solvent system of 100% MeOH, and four fractions were obtained (E8B1–E8B4). Fraction E8B1 (53.2 mg) was purified using semi-preparative HPLC with solvent system of MeOH-H_2O [formic acid 0.1% (v/v)] (34% MeOH) to yield compounds **13** (t_R 37.0 min, 1.3 mg) and **17** (t_R 42.0 min, 2.4 mg). Fraction E8B2

(26.8 mg) was purified using semi-preparative HPLC with a solvent system of MeOH-H_2O [formic acid 0.1% (v/v)] (35% MeOH) to give compounds **14** (t_R 34.0 min, 1.2 mg), **15** (t_R 53.5 min, 1.6 mg), and **16** (t_R 59.0 min, 1.5 mg). Fraction E8B3 (20.6 mg) was purified using semi-preparative HPLC with a solvent system of MeOH-H_2O [formic acid 0.1% (v/v)] (38% MeOH) to yield compound **22** (t_R 20.0 min, 0.3 mg). Fraction E8B4 (18.9 mg) was purified using semi-preparative HPLC with solvent system of MeOH-H_2O (33% MeOH) to yield compounds **9** (t_R 40.5 min, 1.3 mg), **10** (t_R 52.0 min, 1.2 mg), and **11** (t_R 27.5 min, 1.3 mg). Fraction E8C (228.5 mg) was separated on Sephadex LH-20 column using a solvent system of 100% MeOH and five fractions were obtained (E8C1–E8C5). Fraction E8C3 (14.6 mg) was purified using semi-preparative HPLC with a solvent system of MeOH-H_2O [formic acid 0.1% (v/v)] (35% MeOH) to obtain compounds **12** (t_R 33.0 min, 0.7 mg) and **23** (t_R 35.5 min, 0.5 mg). Fraction E8D (103.8 mg) was separated by preparative reversed-phase HPLC with a gradient solvent system of MeCN-H_2O (25–40% MeCN) to give six fractions (E8D1–E8D6). Fraction E8D3 (12.6 mg) and E8D4 (25.1 mg) were combined and separated on Sephadex LH-20 column using a solvent system of MeOH 100% to obtain four fractions (E8D31–E8D34). Fraction E8D32 (17.5 mg) was purified using semi-preparative HPLC with a solvent system of MeOH-H_2O [formic acid 0.1% (v/v)] (46% MeOH) to isolate compound **7** (t_R 29.5 min, 6.3 mg). Fraction E8E (65.4 mg) was separated on Sephadex LH-20 column using a solvent system of 100% MeOH to yield five fractions (E8E1–E8E5). Fraction E8E3 (13.9 mg) was purified using semi-preparative HPLC with a solvent system of MeCN-H_2O [formic acid 0.1% (v/v)] (22% MeCN) to yield compound **8** (t_R 47.5 min, 0.6 mg).

2.3.1. (2R,3S)-2-Ethoxychroman-3,5,7-triol-7-O-β-D-apiofuranoside (1)

Colorless gum; [α]-10.0 (*c* 0.01, MeOH); UV (MeOH) λ_{max} (log ε) 206 (4.2) nm; ECD (MeOH) λ_{max} (Δε) 209 (−17.3), 231 (−7.5), 270 (−9.3) nm; IR (KBr) ν_{max} 3353, 2925, 2839, 1457, 1104, 1023 cm^{-1}; ^1H (800 MHz, CD_3OD) and ^{13}C (200 MHz, CD_3OD) NMR data, see Table 1; ESIMS (positive-ion mode) *m/z*: 381 $[M + Na]^+$. HR-ESIMS (negative-ion mode) *m/z*: 357.1177 $[M - H]^+$ (calcd. for $C_{16}H_{21}O_9$, 357.1186).

2.4. Acid hydrolysis of 1

The absolute configuration of the sugar moiety was determined using a HPLC-UV-based method [22–25]. Compound **1** (0.8 mg) was hydrolyzed in the presence of 1 N HCl at 80 °C for 2 h and EtOAc was used for the extraction. The aqueous layer was neutralized with repeated evaporation under a vacuum evaporator and dissolved in anhydrous pyridine (0.5 mL) with the addition of L-cysteine methyl ester hydrochloride (2 mg). After the reaction mixture was heated at 60 °C for 1.5 h, *o*-tolylisothiocyanate (50 μL) was added and the mixture was kept at 60 °C for 1 h. The reaction product was evaporated under a vacuum evaporator and dissolved in MeOH. After then, the dissolved reaction product was directly analyzed by LC/MS [MeOH/H_2O, 4:1 → 1:1 gradient system (0–30 min), 100% MeOH (31–41 min); 0.3 mL/min] using analytical Kinetex C18 100 Å column (100 mm × 2.1 mm i.d., 5 μm). The sugar moiety from **1** was identified as D-apiofuranose based on the comparison of the retention time of an authentic sample (t_R: D-apiofuranose 27.2 min).

Table 1
^1H (800 MHz) and ^{13}C (200 MHz) NMR data of compound **1** in CD_3OD[a].

No.	1	
	δ_H	δ_C
2	4.95 d (3.0)	100.9 d
3	3.91 dt (3.0, 4.5)	65.9 d
4	2.60 dd (3.0, 17.0); 2.71 dd (4.5, 17.0)	25.4 t
5		158.4 s
6	6.13 d (2.5)	98.5 d
7		158.8 s
8	6.06 d (2.5)	98.3 d
9		154.6 s
10		103.6 s
1′	3.64 m; 3.85 m	65.8 t
2′	1.16 t (7.0)	16.3 q
1″	5.45 d (3.0)	109.6 d
2″	4.12 d (3.0)	79.1 d
3″		81.1 s
4″	3.83 d (10.0); 4.07 d (10.0)	76.2 t
5″	3.59 d (11.4); 3.62 d (11.4)	65.7 t

[a] Assignments based on ^1H–^1H COSY, HSQC, and HMBC. Coupling constants (in Hz) are in parentheses.

2.5. Computational ECD calculation

To acquire the conformational optimization of **1a/1b**, computational DFT calculations were carried out. The first structural energy minimization of **1a/1b** was performed by utilizing Avogadro 1.2.0 with the UFF force field. The ground-state geometries of **1a/1b** were established by Tmolex 4.3.1 with the DFT settings (B3-LYP functional/M3 grid size), geometry optimization options (energy 10^{-6} hartree, gradient norm $|dE/dxyz| = 10^{-3}$ hartree/bohr), and the basis set def-SV (P) for all atoms [26–28]. The calculated ECD spectra of optimized structures were acquired at the B3LYP/DFT functional settings with the basis set def2-TZVPP for all atoms [26–28]. The obtained CD spectra were simulated by overlaying each transition, where σ is the width of the band at 1/e height. ΔE_i and R_i are the excitation energies and the rotatory strengths for transition *i*, respectively. In the present study, the value of σ was 0.10 eV.

$$\Delta \in (E) = \frac{1}{2.297 \times 10^{-39}} \frac{1}{2\pi\sigma} \sum_{A}^{i} \Delta E_i R_i e^{[-(E-\Delta E_i)^2/(2\sigma)^2]}$$

2.6. Computational NMR chemical shift calculations for DP4+ analysis

Conformational searches were performed using the Tmolex 4.3.1 with the DFT settings (B3-LYP functional/M3 grid size), geometry optimization settings (energy 10^{-6} hartree, gradient norm $|dE/dxyz| = 10^{-3}$ hartree/bohr), and the basis set def-SV(P) for all atoms. NMR shielding constants calculations were performed on the optimized ground state geometries at the DFT B3LYP/def-SV(P) level of theory. The NMR chemical shifts of the isomers were obtained by Boltzmann averaging the ^1H NMR and ^{13}C NMR chemical shifts of the stable conformers at 298.15 K. Chemical shift values were calculated using the equation below where δ^x_{calc} is the calculated NMR chemical shift for nucleus *x*, and σ^o is the shielding tensor for the proton and carbon nuclei in tetramethylsilane calculated at the DFT B3LYP/def-SV(P) basis set [29].

$$\delta^x_{calc} = \frac{\sigma^o - \sigma^x}{1 - \sigma^o/10^6}$$

The calculated NMR properties of the optimized structures were averaged based upon their respective Boltzmann populations, and DP4+ probability analysis was facilitated by the Excel sheet (DP4+) provided by Grimblat et al. [30].

2.7. NGF and cell viability assay

In the present study, C6 glioma cells were used to measure the release of NGF into culture medium. C6 cells were seeded in a 24-well plate at a density of 1×10^5 cells/well, cells were treated after 24 h with serum-free Dulbecco's Modified Eagle Medium (DMEM) and the specified concentrations of the compound. After 24 h, the condition medium was collected and centrifuged; NGF produced in C6 glioma

culture supernatants were measured by competitive enzyme-linked immunosorbent assay (ELISA) kits in accordance with the manufacturer's protocol. Untreated control cells were maintained concomitantly. Cell viability was measured using methylthiazolyldiphenyltetrazolium bromide (MTT) assay, as described previously [31–33].

2.8. NO production assay

Murine microglia BV-2 cells were maintained in DMEM supplemented with 10% fetal bovine serum, penicillin (100 U/ml) and streptomycin (100 μg/ml) in a humidified incubator containing 95% air and 5% CO_2 at 37 °C. BV-2 cells were pretreated with the indicated concentration of compounds for 30 min and stimulated with 100 ng/mL LPS for another 24 h. Nitrite, a soluble oxidation product of NO, was measured in the culture media by the Griess reaction [34]. Briefly, the supernatant (50 μL) was harvested and mixed with an equal volume of Griess reagent (1% sulfanilamide, 0.1% N-1-naphthylethylenediamine dihydrochloride in 5% phosphoric acid). The absorbance at 540 nm was measured after 10 min using a microplate reader. Sodium nitrite was used as a standard in the assay. Cell viability was measured using MTT assay, as described previously [31–33].

2.9. Anti-Helicobacter pylori activity

Two strains of *H. pylori* 51 and 43,504 were obtained from *Helicobacter pylori* Korean Type Culture Collection, School of Medicine, Gyeongsang National University, Korea. The strains were cultured under 100% humidity and 10% CO_2 at 37 °C. Brucella broth medium (BD Co., Sparks, MD, USA) was supplemented with 10% horse serum (Gibco, New York, USA). The broth liquid dilution method was used for the determination of minimal inhibitory concentration (MIC). Serial two-fold dilutions of samples and the bacterial colony suspension equivalent to 2.5×10^8 cfu/mL were added to the culture medium and were incubated at 37 °C for 24 h. After incubation, MIC was defined as the lowest concentration of compounds at which bacterial growth was inhibited. Bacterial growth was evaluated by measuring the optical density at 600 nm. Quercetin, metronidazole, and clarithromycin were purchased from Sigma (St. Louis, MO, USA) and used as positive controls.

3. Results and discussion

3.1. Isolation of compounds from the EtOH extract of U. davidiana var. japonica root bark

Phytochemical investigation of the EtOH extract of *U. davidiana* var. *japonica* root bark was performed using successive column chromatography over Diaion HP-20, silica gel, RP-C_{18} silica gel, and Sephadex LH-20 as well as preparative and semi-preparative HPLC combined with LC/MS-based analysis. These procedures resulted in the isolation and the identification of a new chromane derivative (**1**) and 22 known compounds: catechin derivatives (**2–5**), megastigmane glycoside (**6**), dihydrochalcone glycosides (**7** and **8**), flavanone glycosides (**9** and **10**), coumarins (**11** and **12**), lignan derivatives (**13–17**), and phenolic compounds (**18–23**) (Fig. 1).

3.2. Structural elucidation of the isolated compounds

Compound **1** was isolated as a colorless gum with the molecular formula of $C_{16}H_{22}O_9$ (six degrees of unsaturation) as deduced from the negative-ion HR-ESIMS data at *m/z* 357.1177 $[M-H]^-$ (calcd for $C_{16}H_{21}O_9$ 357.1186), and NMR data (Table 1). The IR spectrum of **1** displayed absorption bands for hydroxy (3352 cm^{-1}) and phenyl ring (1565 and 1456 cm^{-1}) functional groups. The ^1H NMR spectrum (Table 1) of **1** showed the presence of a set of aromatic protons at δ_H 6.13 (1H, d, J = 2.5 Hz, H-6) and 6.06 (1H, d, J = 2.5 Hz, H-8). Furthermore, the presence of signals for a methylene at δ_H 2.71 (1H, dd, J = 17.0, 4.5 Hz, H-4b) and 2.60 (1H, dd, J = 17.0, 3.0 Hz, H-4a), and two coupled oxygenated methine protons at δ_H 4.95 (1H, d, J = 3.0 Hz, H-2) and 3.91 (1H, dt, J = 4.5, 3.0 Hz, H-3), were observed. These NMR spectroscopic data suggest a chromane-type derivative as a skeleton of **1** [31]. The presence of an ethoxy group was also indicated by the signal from one methyl group at δ_H 1.16 (3H, t, J = 7.0 Hz, H-2′) and one oxygenated methylene at δ_H 3.85 (1H, m, H-1′b) and 3.64 (1H, m, H-1′a). In addition, the proton signals attributed to sugar moiety including characteristic anomeric [δ_H 5.45 (1H, d, J = 3.0 Hz, H-1″)] and two oxygenated methylene proton signals [δ_H 4.07 (1H, d, J = 10.0 Hz, H-4″b)/3.83 (1H, d, J = 10.0 Hz, H-4″a) and δ_H 3.62 (1H, d, J = 11.4 Hz H-5″b)/3.59 (1H, d, J = 11.4 Hz H-5″a)], were observed. The ^{13}C NMR data of **1** (Table 1) revealed the presence of 16 carbon signals, which were classified with the assistance of HSQC spectrum as five quaternary carbons (δ_C 158.8, 158.4, 154.6, 103.6, and 81.1), including two sp^2 oxygenated quaternary carbons (δ_C 158.8, 158.4, and 154.6) and one sp^3 oxygenated quaternary carbon (δ_C 81.1), one methyl (δ_C 16.3), four methylene (δ_C 76.2, 65.8, 65.7, and 25.4), and six methine (δ_C 109.6, 100.9, 98.5, 98.3, 79.1, and 65.9) groups. These ^{13}C NMR data information support the deduction that compound **1** is composed of chromane-type skeleton, an ethoxy group, and one sugar unit.

The planar structure of **1** was elucidated through 2D NMR analysis (^1H–^1H COSY, HSQC, and HMBC) (Fig. 2). The $^1H-^1H$ COSY correlations starting at H-2, via H-3, ending at H-4 and the HMBC correlations of H-2/C-4 and C-9, H-3/C-10, H-4/C-2, C-5, and C-9, H-6/C-5, C-7, C-8, and C-10, and H-8/C-6, C-7, C-9, and C-10 allowed us to confirm the chromane type skeleton of **1** [35]. The ethoxy group was linked at C-2 by the HMBC correlations from H-2 to C-1′ and from H-1′ to C-2 (Fig. 2). Furthermore, the remaining ^{13}C NMR data combined with the corresponding ^1H NMR data by HSQC experiment indicate the presence of sugar moiety, which was determined to be an apiofuranose by comparing with the previously reported values of apiofuranose [36]. Its position was C-7 of aglycone, based on the important HMBC correlation of H-1″ (δ_H 5.45)/C-7 (δ_C 158.8) (Fig. 2).

The absolute configuration of sugar moiety was determined using a HPLC-UV-based method, [22–25] and acid hydrolysis of **1** was carried out to yield an apiofuranose. The absolute configuration was determined as D-apiofuranose, by the comparison of the retention time of its thiocarbamoyl-thiazolidine derivative of the acid hydrolysate (27.2 min) with that of the standard sample of D-apiofuranose (27.2 min) in LC/MS analysis (Fig. S7), and the coupling constant (J = 3.0 Hz) of anomeric proton signals was indicative of β-form for apiofuranoside. The relative configuration of **1** between H-2 and H-3 was determined through the typical coupling constant (J = 3.0 Hz) as *cis* configuration. In order to confirm the absolute configuration, quantum chemical ECD calculations were performed by the comparison of the experimental ECD spectrum of **1** with the calculated ECD data of two possible enantiomers **1a** (2*R*,3*S*) and **1b** (2*S*,3*R*). However, the ECD calculations did not provide satisfactory conclusion to determine the absolute configuration. Next, the determination of absolute stereochemistry for C-2 and C-3 of **1** was attempted by the gauge-including atomic orbital (GIAO) NMR chemical shifts calculation, followed by DP4+ analysis [30]. The computationally calculated ^1H and ^{13}C NMR chemical shifts of two possible diastereomers **1a** (2*R*,3*S*) and **1b** (2*S*,3*R*) were compared with the experimental values of **1** by utilizing DP4+ probability analysis, which indicated the structural equivalence of **1** to **1a** (2*R*,3*S*) with 100% probability (Fig. S8). In addition, according to the formula $\Delta\delta = \delta_{calcd} - \delta_{exptl}$, the differences ($\Delta\delta$) were determined, and the results are shown in Tables S1 and S2. The correlation coefficient (R^2) obtained by linear regression analysis, largest absolute deviation (LAD), and the mean absolute deviation (MAD) for ^1H NMR data of **1a** (2*R*,3*S*) were 0.9097 (Fig. 3A), 1.37, and 0.33 (Fig. 3B), whereas R^2, LAD, and MAD values for those of **1b** (2*S*,3*R*) were 0.5309, 3.84, and 0.59, respectively. In terms of ^{13}C NMR data, the correlation coefficient (R^2) obtained by linear regression analysis, largest absolute deviation (LAD), and the mean absolute deviation (MAD) for **1a** (2*R*,3*S*)

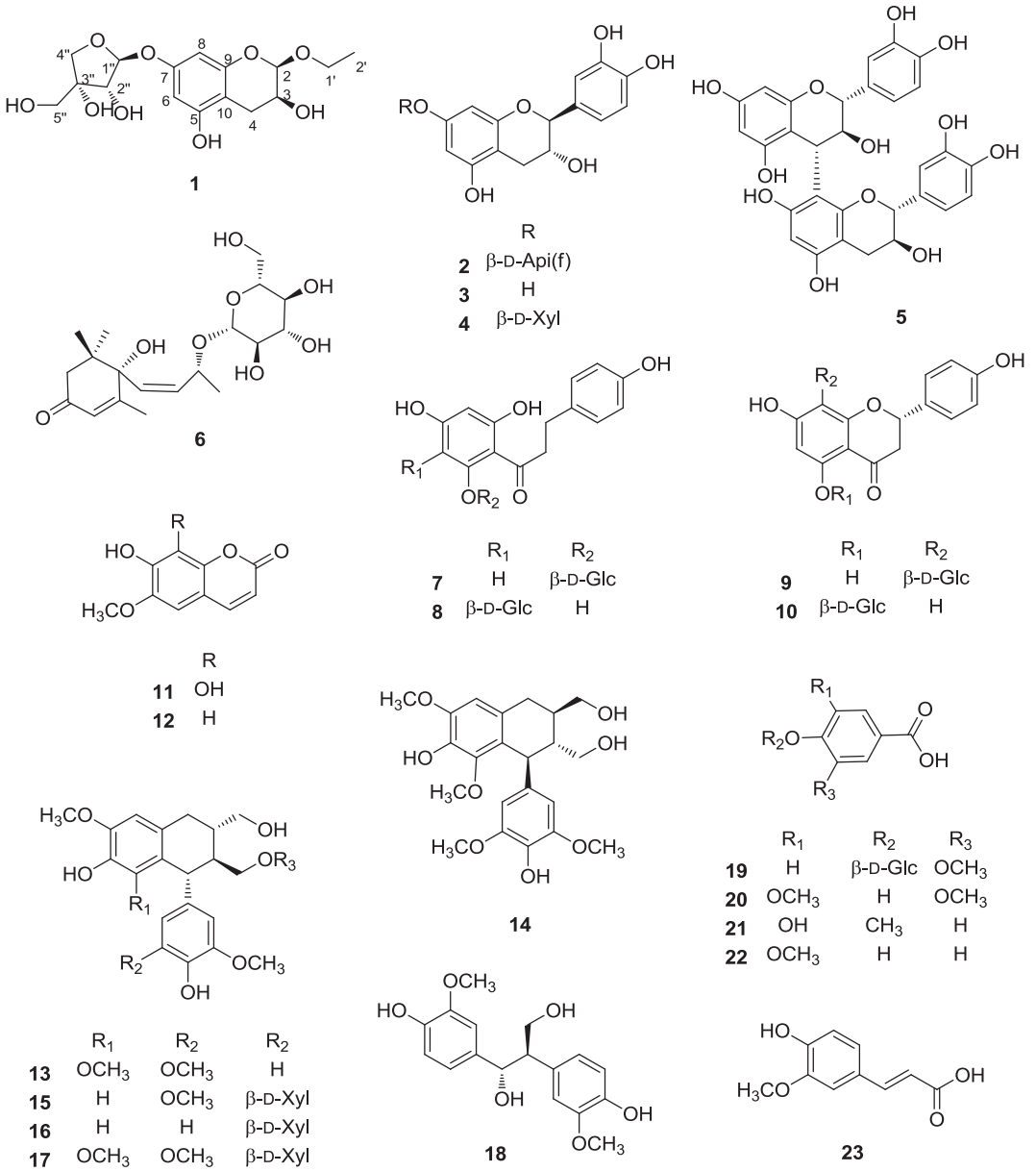

Fig. 1. Chemical structures of compounds **1–23** isolated from *U. davidiana* var. *japonica*. Api(f), apiofuranosyl; Xyl, xylopyranosyl; Glc, glucopyranosyl.

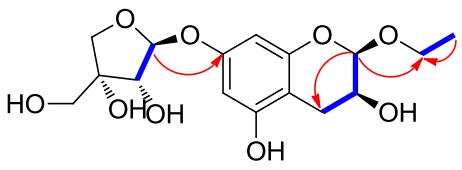

Fig. 2. ^{1}H–^{1}H COSY (bold lines) and key HMBC (red arrows) correlations for compound **1**.

were 0.9948 (Fig. 3C), 14.33, and 3.78 (Fig. 3D), whereas R^2, LAD, and MAD values for **1b** (2*S*,3*R*) were 0.9942, 15.48, and 3.86, respectively. The obtained data supported the absolute stereochemistry for C-2 and C-3 to be 2*R* and 3*S*, respectively. Accordingly, the structure of compound **1** was determined as (2*R*,3*S*)-2-ethoxychroman-3,5,7-triol-7-*O*-β-D-apiofuranoside.

Other 22 known compounds were identified as (-)-catechin-7-*O*-β-D-apiofuranoside (**2**) [37], (-)-catechin (**3**) [38], (-)-catechin-7-*O*-β-D-xylopyranoside (**4**) [39], procyanidin B3 (**5**) [40,41], (+)-*cis*-roseoside (**6**) [42,43], phloridzin (**7**) [44], nothofagin (**8**) [45], isohemiphloin (**9**) [46], helichrysin A (**10**) [47-49], fraxetin (**11**) [50], scopoletin (**12**) [51,52], (-)-lyoniresinol (**13**) [50], (+)-lyoniresinol (**14**) [50], (+)-5′-methoxy-isolariciresinol-9′-*O*-β-D-xylopyranoside (**15**) [11], (-)-isolariciresinol 9′-*O*-β-D-xylopyranoside (**16**) [11,53], nudiposide (**17**) [54,55], (1*S*,2*R*)-1,2-*bis*(4-hydroxy-3-methoxyphenyl)-1,3-propanediol (**18**) [56], 4-*O*-β-D-glucopyranosyl vanillic acid (**19**) [57], syringic acid (**20**) [58], isovanillic acid (**21**) [59], vanillic acid (**22**) [51,60], and *trans*-ferulic acid (**23**) [61,62] by comparing their NMR spectroscopic spectra data with those from literature, and also by LC/MS analysis (Fig. 1). Among the isolates, compounds **7–14**, **16**, and **18–23** were isolated from *U. davidiana* var. *japonica* for the first time, and compounds **7–14**, **16**, **18–19**, **21**, and **23** were first reported in plants of the Ulmaceae family.

3.3. Biological activities

3.3.1. Effect of the isolated compounds on NGF production

U. davidiana var. *japonica* has been known to possess anti-inflammatory activity [14]; however, its role to inhibit

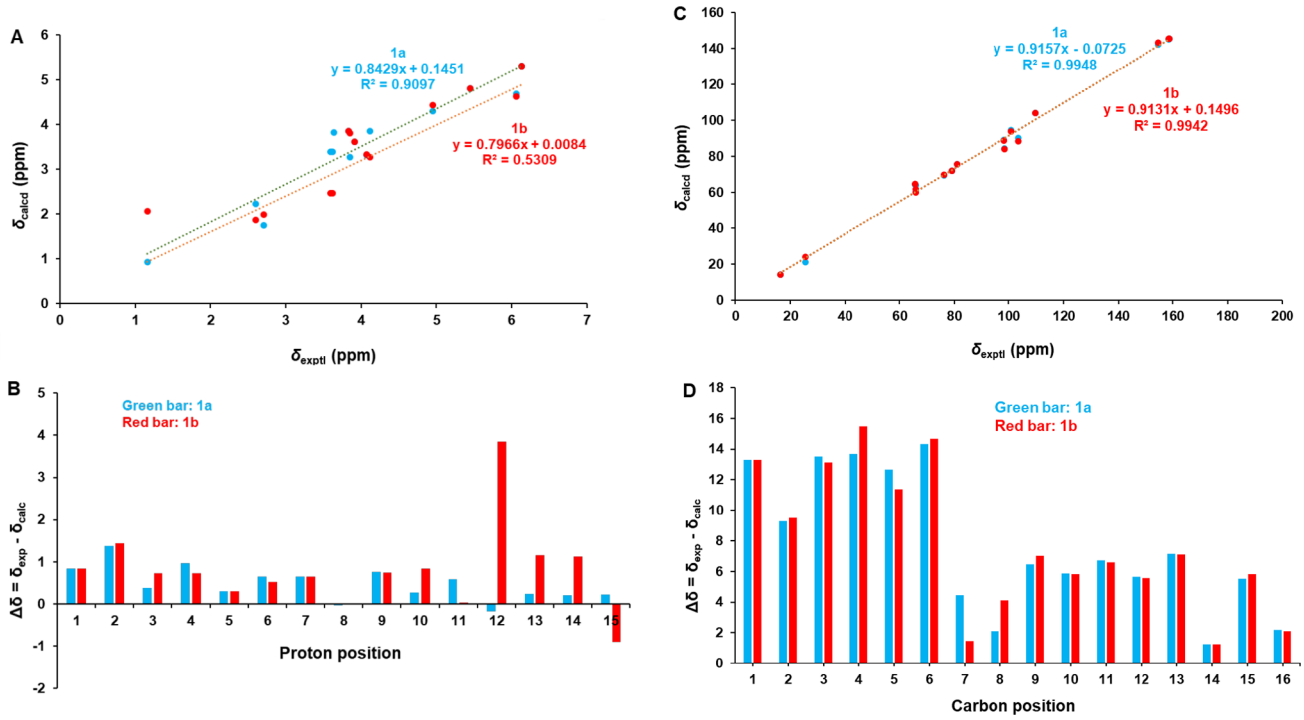

Fig. 3. (A) Regression analysis of experimental versus computationally calculated ^{1}H NMR chemical shifts of **1a** (2*R*,3*S*) and **1b** (2*S*,3*R*) with linear fitting shown as a line. (B) Relative chemical shift errors between calculated and experimental ^{1}H NMR data for **1a** (2*R*,3*S*) and **1b** (2*S*,3*R*). (C) Regression analysis of experimental versus computationally calculated ^{13}C NMR chemical shifts of **1a** (2*R*,3*S*) and **1b** (2*S*,3*R*) with linear fitting shown as a line. (D) Relative chemical shift errors between calculated and experimental ^{13}C NMR data for **1a** (2*R*,3*S*) and **1b** (2*S*,3*R*).

neuroinflammation in neurodegenerative diseases (ND) such as Alzheimer's disease, Parkinson's disease, and multiple sclerosis is unknown. Neuroinflammation, relatively due to uncontrolled activation of microglia, is associated with the pathogenesis of ND. NO is an inflammatory mediator in CNS and the overproduction of NO can result in neuronal damage [63]. Recently, it was reported that neurotrophic factors such as NGF, has the potential to regulate the survival, proliferation, migration, and differentiation of cells in the nervous system [64,65]. Phytochemicals that induce the secretion of neurotrophins such as NGF will be able to protect neurons against degeneration caused by uncontrolled neuroinflammation.

All the isolates (**1–23**) were evaluated for their neuroprotective effect by determining the secretion of NGF using C6 glioma cells as a model system of astrocytes (Table 2). Of the tested compounds at 20 μM, compounds **1**, **8**, and **20** were more potent stimulants of NGF release, with stimulation levels of 147.04 ± 4.87, 206.27 ± 6.70, and 143.70 ± 0.88%, respectively compared with the positive control, 6-shogaol, which had a value of 141.62 ± 4.55%. Compounds **7**, **10**, **16**, and **22** exhibited moderate activity with stimulation levels ranging from 130.20 ± 4.16% to 134.15 ± 6.83%.

3.3.2. *Effect of the isolated compounds on NO production*

Activated microglia causes the excessive production of inflammatory mediators such as NO, which play a key role in neurodegeneration [66]. Thus, the inhibitory effects of all the isolates on NO production in LPS-activated murine microglia BV-2 cells were evaluated (Table 3). Compounds **11**, **14**, and **19** exhibited significant inhibitory activity against NO production with IC_{50} values of 18.72, 12.31, and 21.40 μM, respectively (positive control, L-NMMA: IC_{50} = 21.73 μM), whereas compounds **13**, **17**, and **20** showed moderate inhibitory effect with IC_{50} values of 24.93–28.21 μM. Particularly, the results indicate that compounds **11** and **14** exhibited better potency than a well-known iNOS inhibitor, L-NMMA (Table 3).

Table 2
Effects of compounds **1–23** on NGF secretion in C6 cells.

Compounds	NGF Secretion (% of Ctl)[a]	Cell viability[b]
1	147.04 ± 4.87	105.22 ± 5.44
2	84.39 ± 2.83	108.53 ± 0.33
3	71.02 ± 0.01	103.84 ± 4.10
4	71.61 ± 0.10	107.38 ± 2.14
5	86.87 ± 8.25	112.81 ± 5.05
6	95.82 ± 2.70	98.13 ± 4.12
7	130.20 ± 4.16	103.45 ± 9.36
8	206.27 ± 6.70	94.55 ± 4.82
9	106.20 ± 0.01	107.70 ± 4.95
10	131.39 ± 8.26	95.05 ± 0.85
11	104.14 ± 0.45	107.29 ± 2.99
12	105.62 ± 7.11	104.94 ± 5.05
13	109.02 ± 15.94	92.35 ± 3.26
14	98.86 ± 3.60	100.10 ± 4.50
15	83.32 ± 5.51	106.01 ± 1.96
16	131.29 ± 7.47	104.56 ± 0.39
17	113.60 ± 5.20	103.61 ± 5.98
18	101.62 ± 3.38	91.42 ± 2.72
19	96.43 ± 3.24	112.68 ± 0.39
20	143.70 ± 0.88	100.77 ± 2.59
21	103.04 ± 0.84	111.63 ± 1.10
22	134.15 ± 6.83	97.03 ± 4.74
23	125.13 ± 4.12	111.10 ± 1.01
6-shogaol[c]	141.62 ± 4.55	113.24 ± 8.08

[a] C6 cells were treated with 20 μM of each compound. After 24 h, the level of NGF secreted in the C6-conditioned medium was measured by ELISA. The level of secreted NGF is expressed as the percentage of the untreated control (Ctl, set as 100%).

[b] Cell viability after treatment with 20 μM of each compound was determined by MTT assay and is expressed as percentage (%). Results are the means of three independent experiments, and the data are expressed as mean ± SD.

[c] Positive control substance.

Table 3
Inhibitory effect of compounds **1**–**23** on NO production in LPS-activated BV-2 cells.

Compounds	IC_{50} (μM)[a]	Cell viability[b]
1	81.37	103.53 ± 1.55
2	> 500	77.30 ± 6.03
3	37.10	99.95 ± 6.30
4	37.26	91.31 ± 4.71
5	70.11	80.08 ± 3.91
6	99.93	84.03 ± 3.29
7	80.53	89.18 ± 7.09
8	241.75	92.56 ± 3.78
9	42.85	114.52 ± 2.27
10	37.53	111.49 ± 2.45
11	18.72	102.51 ± 1.14
12	47.69	108.38 ± 1.12
13	27.01	97.27 ± 9.05
14	12.31	94.57 ± 0.90
15	> 500	101.44 ± 6.37
16	33.24	96.20 ± 5.43
17	28.21	89.40 ± 2.51
18	89.72	105.32 ± 3.94
19	21.40	88.67 ± 2.77
20	24.93	105.57 ± 3.42
21	72.33	106.14 ± 1.15
22	72.09	103.01 ± 8.90
23	> 500	105.96 ± 3.42
L-NMMA[c]	21.73	107.74 ± 4.22

[a] IC_{50} value of each compound was defined as the concentration (μM) that caused 50% inhibition of NO production in LPS-activated BV-2 cells.
[b] Cell viability following treatment with 20 μM of each compound was determined using the MTT assay and is expressed as a percentage (%). Data are expressed as the mean ± SD of three independent experiments.
[c] Positive control substance.

Table 4
Anti-*Helicobacter pylori activity* of the selected compounds **1**, **11**, **18**, and **20**.

Compounds	MIC (μM)	
	H. pylori strain 51	*H. pylori* strain 43,504
1	25	50
11	50	25
18	25	25
20	25	50
quercetin[a]	50	50
metronidazole[a]	12.5	12.5
clarithromycin[a]	0.5	0.5

[a] Positive controls.

3.3.3. Anti-H. pylori activity

The root bark of this plant has been used as a traditional medicine in Korea for the treatment of gastroenteric disorders including gastritis and gastric cancer. *Helicobacter pylori* is well-known to play an etiological role in these diseases [62,67], hence, all isolated compounds (**1–23**) were tested for anti-bacterial activity against two strains of *H. pylori*. Broth dilution method was used for the determination of minimal inhibitory concentrations (MIC). Compounds **1**, **11**, **18**, and **20** showed anti-*H. pylori* activity with MIC values of 25 or 50 μM against the two strains, *H. pylori* 51 and 43,504 (Table 4); and their activities were comparable to that of the positive control—quercetin, a natural product. However, the others failed to show anti-bacterial activity. Although the anti-*H. pylori* activity of syringic acid (**20**) has been reported [68], this is the first report of the growth inhibitory activity of compounds **1**, **11**, and **18**.

4. Conclusions

In this study, we provide further scientific evidence to support the traditional use of *U. davidiana* var. *japonica* root bark (yugeunpi in Korea) for the treatment of gastroenteric and inflammatory disorders. Phytochemical analysis of the EtOH extract of *U. davidiana* var. *japonica* root bark led to the isolation and characterization of a new chromane derivative (**1**) and 22 known compounds (**2–23**). The present results suggest that bioactive compounds **1**, **8**, and **20** may be useful in the development of neurotrophic agents, and compounds **11**, **14**, and **19** may exert functional roles in the mitigation of neurodegenerative diseases. Compound **20** exhibited bifunctional roles—the initiation of NGF secretion and the inhibition of NO production. This suggest that the bioactive compounds of *U. davidiana* var. *japonica* can inhibit neuroinflammation and increase NGF secretion; hence, they can be utilized as therapeutic agents in neurodegenerative disorders. In addition, compounds **1**, **11**, **18**, and **20** possibly contribute to the efficacy of this medicinal plant in gastrointestinal disorders through the inhibition of the growth of *H. pylori*.

Declaration of Competing Interest

The authors declare no competing financial interests.

Acknowledgements

This work was supported by the National Research Foundation of Korea (NRF) grant funded by the Korea government (MSIT) (2018R1A2B2006879) and the R&D Program for Forest Science Technology (Project No. 2017036A00-1719-BA01) provided by Korea Forest Service (Korea Forestry Promotion Institute). We would like to thank Dr. Young Hye Kim (Korea Basic Science Institute) for ESI-MS analysis.

Appendix A. Supplementary material

Supplementary data to this article can be found online at https://doi.org/10.1016/j.bioorg.2019.103145.

References

[1] J.H. Pan, Y. Lim, J.H. Kim, W. Heo, K.Y. Lee, H.J. Shin, J. Kim, J.H. Lee, Y.J. Kim, Root bark of *Ulmus davidiana* var. *japonica* restrains acute alcohol-induced hepatic steatosis onset in mice by inhibiting ROS accumulation, PLoS One 12 (2017) e0188381.
[2] N.D. Hong, Y.S. Rho, N.J. Kim, J.S. Kim, A study on efficacy of Ulmi cortex, Kor. J. Pharmacogn. 21 (1990) 217–222.
[3] S.J Lee, Korean Folk Medicine. Monographs, Series No. 3, Seoul National University Press: Seoul, 1996.
[4] M.K. Lee, Y.C. Kim, Five novel neuroprotective triterpene esters of *Ulmus davidiana* var. *japonica*, J. Nat. Prod. 64 (2001) 328–331.
[5] B.W. Son, J.H. Park, O.P. Zee, Catechin glycoside from *Ulmus davidiana*, Arch. Pharm. Res. 21 (1989) 219–222.
[6] K.S. Kim, S.D. Lee, K.H. Kim, S.Y. Kil, K.H. Chung, C.H. Kim, Suppressive effects of a water extract of *Ulmus davidiana* Planch (Ulmaceae) on collagen-induced arthritis in mice, J. Ethnopharmacol. 97 (2005) 65–71.
[7] H.J. Jung, H.J. Jeon, E.J. Lim, E.K. Ahn, Y.S. Song, S. Lee, K.H. Shin, C.J. Lim, E.H. Park, Anti-angiogenic activity of the methanol extract and its fraction of *Ulmus davidiana* var. *japonica*, J. Ethnopharmacol. 112 (2007) 406–409.
[8] Y. Lee, H. Park, H.S. Ryu, M. Chun, S. Kang, H.S. Kim, Effects of elm bark (*Ulmus davidiana* var. *japonica*) extracts on the modulation of immunocompetence in mice, J. Med. Food 10 (2007) 118–125.
[9] C.S. Kim, J.M. Lee, C.O. Choi, S.B. Park, T.J. Eom, Chemical analysis and isolation of antibacterial compound from Ulmus species (II): isolation and chemical structure of antibacterial compound, Mokchae Konghak 31 (2003) 16–21.
[10] J.P. Kim, W.G. Kim, H. Koshino, J. Jung, I.D. Yoo, Sesquiterpene-*O*-naphthaquinones from the root bark of *Ulmus davidiana*, Phytochemistry 43 (1996) 425–430.
[11] M.K. Lee, S.H. Sung, H.S. Lee, J.H. Cho, Y.C. Kim, Lignan and neolignan glycosides from *Ulmus davidiana* var. *japonica*, Arch. Pharm. Res. 24 (2001) 198–201.
[12] M.S. Zheng, Y.K. Lee, Y. Li, K. Hwangbo, C.S. Lee, J.R. Kim, S.K.S. Lee, H.W. Chang, J.K. Son, Inhibition of DNA topoisomerases I and II and cytotoxicity of compounds from *Ulmus davidiana* var. *japonica*, Arch. Pharm. Res. 33 (2010) 1307–1315.
[13] G.Y. Lee, D.S. Jang, J. Kim, C.S. Kim, Y.S. Kim, J.H. Kim, J.S. Kim, Flavan-3-ols from *Ulmus davidiana* var. *japonica* with inhibitory activity on protein glycation, Planta. Med. 74 (2008) 1800–1802.
[14] Y.C. Kim, M.K. Lee, S.H. Sung, S.H. Kim, Sesquiterpenes from *Ulmus davidiana* var. *japonica* with the inhibitory effects on lipopolysaccharide-induced nitric oxide production, Fitoterapia 78 (2007) 196–199.

[15] J.S. Yu, D.H. Lee, S.R. Lee, J.W. Lee, C.I. Choi, T.S. Jang, K.S. Kang, K.H. Kim, Chemical characterization of cytotoxic indole acetic acid derivative from Mulberry fruit (*Morus alba* L.) against human cervical cancer, Bioorg. Chem. 76 (2018) 28–36.

[16] S. Lee, E. Choi, S.M. Yang, R. Ryoo, E. Moon, S.H. Kim, K.H. Kim, Bioactive compounds from sclerotia extract of *Poria cocos* that control adipocyte and osteoblast differentiation, Bioorg. Chem. 81 (2018) 27–34.

[17] D. Lee, D.S. Lee, K. Jung, G.S. Hwang, H.L. Lee, N. Yamabe, H.J. Lee, D.W. Eom, K.H. Kim, K.S. Kang, Protective effect of ginsenoside Rb1 against tacrolimus-induced nephrotoxicity in renal proximal tubular LLC-PK1 cells, J. Ginseng Res. 42 (2018) 75–80.

[18] J.S. Yu, J. Baek, H.B. Park, E. Moon, S.Y. Kim, S.U. Choi, K.H. Kim, A new rearranged eudesmane sesquiterpene and bioactive sesquiterpenes from the twigs of *Lindera glauca* (Sieb. et Zucc.) blume, Arch. Pharm. Res. 39 (2016) 1628–1634.

[19] S.C. Baek, E. Choi, H.J. Eom, M.S. Jo, S. Kim, H.M. So, S.H. Kim, K.S. Kang, K.H. Kim, LC/MS-based analysis of bioactive compounds from the bark of *Betula platyphylla* var. *japonica* and their effects on regulation of adipocyte and osteoblast differentiation, Nat. Prod. Sci. 24 (2018) 235–240.

[20] J.S. Yu, H.S. Roh, K.H. Baek, S. Lee, S. Kim, H.M. So, E. Moon, C. Pang, T.S. Jang, K.H. Kim, Bioactivity-guided isolation of ginsenosides from Korean red ginseng with cytotoxic activity against human lung adenocarcinoma cells, J. Ginseng Res. 42 (2018) 562–570.

[21] H.M. So, H.J. Eom, D. Lee, S. Kim, K.S. Kang, I.K. Lee, K.H. Baek, J.Y. Park, K.H. Kim, Bioactivity evaluations of betulin identified from the bark of *Betula platyphylla* var. *japonica* for cancer therapy, Arch. Pharm. Res. 41 (2018) 815–822.

[22] T. Tanaka, T. Nakashima, T. Ueda, K. Tomii, I. Kouno, Facile discrimination of aldose enantiomers by reversed-phase HPLC, Chem. Pharm. Bull. 55 (2007) 899–901.

[23] M.A. Muhit, K. Umehara, K. Mori-Yasumoto, H. Noguchi, Furofuran lignan glucosides with estrogen-inhibitory properties from the Bangladeshi medicinal plant *Terminalia citrina*, J. Nat. Prod. 79 (2016) 1298–1307.

[24] Y.W. Ge, C. Tohda, S. Zhu, Y.M. He, K. Yoshimatsu, K. Komatsu, Effects of oleanane-type triterpene saponins from the leaves of *Eleutherococcus senticosus* in an axonal outgrowth assay, J. Nat. Prod. 79 (2016) 1834–1841.

[25] B. Odonbayer, T. Murata, J. Batkhuu, K. Yasunaga, R. Goto, K. Sasaki, Antioxidant flavonols and phenolic compounds from *Atraphaxis frutescens* and their inhibitory activities against insect Phenoloxidase and mushroom tyrosinase, J. Nat. Prod. 79 (2016) 3065–3071.

[26] K.B. Kang, H.W. Kim, J.W. Kim, W.K. Oh, J. Kim, S.H. Sung, Catechin-bound Ceanothane-type triterpenoid derivatives from the roots of *Zizyphus jujuba*, J. Nat. Prod. 80 (2017) 1048–1054.

[27] K. Kusakabe, Y. Honmura, S. Uesugi, A. Tonouchi, H. Maeda, K. Kimura, H. Koshino, M. Hashimoto, Neomacrophorin X, a [4.4.3]propellane-type Meroterpenoid from *Trichoderma* sp. 1212–03, J. Nat. Prod. 80 (2017) 1484–1492.

[28] S.R. Lee, H.B. Park, K.H. Kim, Highly sensitive, simple, and cost/time-effective method to determine the absolute configuration of a secondary alcohol using competing enantioselective acylation coupled with LC/MS, Anal. Chem. 90 (2018) 13212–13216.

[29] S.G. Smith, J.M. Goodman, Assigning stereochemistry to single diastereoisomers by GIAO NMR calculation: the DP4 probability, J. Am. Chem. Soc. 132 (2010) 12946–12959.

[30] N. Grimblat, M.M. Zanardi, A.M. Sarotti, Beyond DP4: an improved probability for the stereochemical assignment of isomeric compounds using quantum chemical calculations of NMR shifts, J. Org. Chem. 80 (2015) 12526–12534.

[31] X. Wang, G.Y. Su, C. Zhao, F.Z. Qu, P. Wang, Y.Q. Zhao, Anticancer activity and potential mechanisms of 1C, a ginseng saponin derivative, on prostate cancer cells, J. Ginseng Res. 42 (2018) 133–143.

[32] Q.M. Thi Ngo, T.Q. Cao, M.H. Woo, B.S. Min, K.Y. Weon, Cytotoxic triterpenoids from the fruits of *Ligustrum japonicum*, Nat. Prod. Sci. 24 (2018) 93–98.

[33] L.S. Aisyah, Y.F. Yun, T. Herlina, E. Julaeha, A. Zainuddin, I. Nurfarida, A.T. Hidayat, U. Supratman, Y. Shiono, Flavonoid compounds from the leaves of *Kalanchoe prolifera* and their cytotoxic activity against P-388 murine leukimia cells, Nat. Prod. Sci. 23 (2017) 139–145.

[34] C.S. Kim, L. Subedi, S.Y. Kim, S.U. Choi, K.H. Kim, K.R. Lee, Diterpenes from the trunk of *Abies holophylla* and their potential neuroprotective and anti-inflammatory activities, J. Nat. Prod. 79 (2016) 387–394.

[35] P. Marisin, N.S. Pablo, L. Jose, P. Lopez, V. Yelkaira, R. Nelson, O. Dionisio, C. Mireya, S.F. Arturo, P.G. Mahabir, Cytotoxic and antimicrobial benzophenones from the leaves of *Tovomita longifolia*, J. Nat. Prod. 69 (2006) 410–413.

[36] M.J. Jung, S.I. Heo, M.H. Wang, Free radical scavenging and total phenolic contents from methanolic extracts of *Ulmus davidiana*, Food Chem. 108 (2008) 482–487.

[37] M.K. Na, R.B. An, S.M. Lee, B.S. Min, Y.H. Kim, K.H. Bae, S.S. Kang, Antioxidant compounds from the stem bark of *Sorbus commixta*, Nat. Prod. Sci. 8 (2002) 26–29.

[38] A. Nahrstedt, P. Proksch, E.E. Conn, (-)-Catechin, flavonol glycosides and flavones from *Chamaebatia foliolosa*, Phytochemistry 26 (1987) 1546–1547.

[39] H. Otsuka, E. Hirata, T. Shizato, Y. Takeda, Isolation of lignan glucosides and neolignan sulfate from the leaves of *Glochidion zeylanicum* (Gaertn) A. Juss, Chem. Pharm. Bull. 48 (2000) 1084–1086.

[40] N. Kohler, V. Wray, P. Winterhalter, Preparative isolation of procyanidins from grap seed extracts by highspeed counter-current chromatography, J. Chromatogr. A 1177 (2008) 114–125.

[41] I. Tarascou, K. Barathieu, Y. Andr, I. Pianet, E.J. Dufourc, E. Fouquet, An improved synthesis of procyanidin dimers: regio- and stereocontrol of the interflavan bond, Eur. J. Org. Chem. 23 (2006) 5367–5377.

[42] A. Pabst, D. Barron, E. Semon, P. Schreier, Two diastereomeric 3-oxo-α-ionol-β-glucosides from raspberry fruit, Phytochemistry 31 (1992) 1649–1652.

[43] H. Achenbach, R. Waibel, B. Raffelsberger, A.M. Ivan, Iridoid and other constituents of *Canthium subcordatum*, Phytochemistry 20 (1981) 1591–1595.

[44] Y. Takada, K. Machida, M. Kikuchi, Studies on the constituents of Rodgersia podophylla A. Gray. II, J. Tohoku Pharm. Univ. 50 (2003) pp. 89–93.

[45] A. Yepremyan, B. Salehani, T.G. Minehan, Concise total syntheses of aspalathin and nothofagin, Org. Lett. 12 (2010) 1580–1583.

[46] L. Velozo, B. Da Silva, E. Da Silva, J. Parente, Constituents from the roots of *Bowdichia virgilioides*, Fitoterapia 70 (1999) 532–535.

[47] L.F. Ibrahim, W.M. El Senousy, U.W. Hawas, NMR spectral analysis of flavonoids from *Chrysanthemum coronarium*, Chem. Nat. Comp. 43 (2007) 659–662.

[48] S.R. Werner, J.A. Morgan, Expression of a Dianthus flavonoid glucosyltransferase in *Saccharomyces cerevisiae* for whole-cell biocatalysis, J. Biotechnol. 142 (2009) 233–241.

[49] Y. Ding, Y. Xiong, B. Zhou, M. Deng, K. Deng, Isolation and structural identification of flavonoids from *Aurantii Fructus*, China J. Chin. Mater. Med. 40 (2015) 2352–2356.

[50] L. Li, N.P. Seeram, Maple syrup phytochemicals include lignans, coumarins, a stilbene, and other previously unreported antioxidant phenolic compounds, J. Agric. Food Chem. 58 (2010) 11673–11679.

[51] B.B. Zhang, Y. Dai, Z.X. Liao, Chemical constituents of *Saussurea eopygmaea*, Chin. J. Nat. Med. 9 (2011) 33–37.

[52] M.K. Bhatt, K.K. Dholwani, A.K. Saluja, Isolation and structure elucidation of scopoletin from *Ipomoea reniformis* (Convolvulaceae), J. Appl. Pharm. Sci. 01 (2011) 138–144.

[53] L.N. Lundgren, T. Popoff, O. Theander, Dilignol glycosides from needels of *Picea abies*, Phytochemistry 20 (1981) 1967–1969.

[54] S.M. Inoshiri, H. Kohda, H. Otsuka, K. Yamasaki, Aromatic glycosides from *Berchemia racemosa*, Phytochemistry 26 (1987) 2811–2814.

[55] E. Smite, H. Pan, L.N. Lundgren, Lignan glycosides from inner bark of *Betula pendula*, Phytochemistry 40 (1995) 341–343.

[56] K. Yoshikawa, N. Mimura, S. Arihara, Isolation and absolute structures of enantiomeric 1,2-*bis*(4-hydroxy-3-methoxyphenyl)-1,3-propanediol-1-*O*-glucosides from the bark of *Hovenia trichocarpa*, J. Nat. Prod. 61 (1998) 1137–1139.

[57] C.B. Cui, Y. Tezuka, H. Yamashita, T. Kikuchi, H. Nakano, T. Tamaoki, J.H. Park, Constituents of a fern, *Davallia mariesii* Moore. V. Isolation and structures of *Davallin*, a new tetrameric proanthocyanidin, and two new phenolic glycosides, Chem. Pharm. Bull. 41 (1993) 1491–1497.

[58] S.M. Pan, H.Y. Ding, W.L. Chang, H.C. Lin, Phenols from the aerial parts of *Leonurus sibiricus*, Chin. Pharm. J. 58 (2006) 35–40.

[59] H. Gao, A. Sui, Y. Chen, X. Zhang, L. Wu, Chemical constituents of *Dioscorea bulbifera* L, J. China Pharm. Univ. 20 (2003) 178–180.

[60] A. Jerezano, F. Jiménez, M. del Carmen Cruz, L.E. Montiel, F. Delgado, J. Tamariz, New approach for the construction of the coumarin frame and application in the total synthesis of natural products, Helv. Chim. Acta 94 (2011) 185–198.

[61] J. Guo, J. Zhang, W. Wang, T. Liu, Z. Xin, Isolation and identification of bound compounds from corn bran and their antioxidant and angiotensin I-converting enzyme inhibitory activities, Eur. Food Res. Technol. 241 (2015) 37–47.

[62] S. Prachayasittikul, S. Suphapong, A. Worachartcheewan, R. Lawung, S. Ruchirawat, V. Prachayasittikul, Bioactive metabolites from *Spilanthes acmella* Murr. Molecules 14 (2009) 850–867.

[63] C.S. Kim, M. Bae, J. Oh, L. Subedi, W.S. Suh, S.Z. Choi, M.W. Son, S.Y. Kim, S.U. Choi, D.C. Oh, K.R. Lee, Anti-neurodegenerative biflavonoid glycosides from *Impatiens balsamina*, J. Nat. Prod. 80 (2017) 471–478.

[64] J.M. Cha, W.S. Suh, T.H. Lee, L. Subedi, S.Y. Kim, K.R. Lee, Phenolic glycosides from *Capsella bursa-pastoris (L.)* Medik and their anti-inflammatory activity, Molecules 22 (2017) 1023.

[65] T.L. Nguyen, C.K. Kim, J.H. Cho, K.H. Lee, J.Y. Ahn, Neuroprotection signaling pathway of nerve growth factor and brain-derived neurotrophic factor against staurosporine induced apoptosis in hippocampal H19–7 cells, Exp. Mol. Med. 42 (2010) 583.

[66] L. Subedi, R. Venkatesan, S.Y. Kim, Neuroprotective and anti-inflammatory activities of allyl isothiocyanate through attenuation of JNK/NF-κB/TNF-α signaling, Int. J. Mol. Sci. 18 (2017) 1423.

[67] W.D. Chey, B.C.Y. Wong, American college of gastroenterology guideline on the management of *Helicobacter pylori* infection, Am. J. Gastroenterol. 102 (2007) 1808–1825.

[68] M.N. Siddaraju, S.M. Dharmesh, Inhibition of gastric H+, K+-ATPase and Helicobacter pylori growth by phenolic antioxidants of *Curcuma amada*, J. Agr. Food Chem. 55 (2007) 7377–7386.